Nuclear import and activity of histone deacetylase in *Xenopus* oocytes is regulated by phosphorylation

David A. Smillie, Alexander J. Llinas, James T. P. Ryan, Graham D. Kemp and John Sommerville*

Division of Cell and Molecular Biology, School of Biology, University of St Andrews, St Andrews, Fife KY16 9TS, UK

*Author for correspondence (e-mail: js15@st-and.ac.uk)

Accepted 24 Novemer 2003
Journal of Cell Science 117, 1857-1866 Published by The Company of Biologists 2004
doi:10.1242/jcs.01008

Summary

Most of the histone deacetylase (HDAC) activity detected in oocytes and early embryos of *Xenopus* can be accounted for by the presence of a protein complex that contains the maternal HDACm protein. This complex appears to fulfil the conditions required of a 'deposition' histone deacetylase, its primary function being to deacetylate the core histones incorporated into newly-synthesized chromatin during the rapid cell cycles leading up to blastula. A major event in the assembly and accumulation of the HDAC complex is the translocation of the HDACm protein into the germinal vesicle during oogenesis. Here we examine the features of HDACm that are responsible for its nuclear uptake and enzyme activity, identifying the charged C-terminal domain as a target for modification by phosphorylation. Whereas, one phosphorylation site lying within the putative nuclear localization signal, T445, is required for efficient nuclear import of a GST-carboxy-tail fusion, two others, S421 and S423, appear to effect release from the import receptors. Although overexpression of recombinant HDACm in oocytes leads to premature condensation of endogenous chromatin, this effect is abrogated in vivo by mutation of S421A and S423A. Thus, both translocation and activity of HDACm appear to be regulated by specific phosphorylation events. These results have implications for techniques involving the transfer of somatic nuclei into enucleated oocytes.

Key words: Histones/chromatin, Protein phosphorylation, Nuclear import

Introduction

Histone deacetylases (HDACs) repress transcription by deacetylating selected lysines in the N-terminal tails of nucleosomal histones, leading to chromatin remodelling. This activity is dependent upon the interaction of HDACs with other proteins to form complexes which often target chromatin sites through binding to transcription factors at specific gene promoters or to DNA-binding proteins within defined chromatin domains (Marmorstein, 2001; Turner, 2000). Other aspects of HDAC function, for instance the effects that post-translational modifications might have on HDAC localization and interaction with cellular structure (Kouzarides, 2000; Li et al., 1996), have received relatively little attention.

Oocytes and early embryos provide favourable material to examine de novo assembly of HDAC complexes and to identify factors that influence their cellular distribution through meiosis and the rapid mitotic cleavages leading to blastula. To fuel this massive expansion in chromatin (~4000-fold in 4 hours), large pools of core histones are accumulated in oocytes in forms modified for optimal assembly of nucleosomes: histone H4, for instance, is stored in the germinal vesicle (GV) as a diacetylated form (Dimitrov et al., 1993). A maternal histone deacetylase, HDACm, is also accumulated during *Xenopus* oogenesis (Ladomery et al., 1997; Ryan et al., 1999), to be used eventually to deacetylate core histones after they have been assembled into embryonic chromatin (Almouzni et al., 1994; Dimitrov et al., 1993). This global deacetylation is thought not only to stabilize nucleosomal organization (Wolffe, 1994), but also 'wipes clean' the embryonic chromatin to allow it to be reprogrammed by site specific acetylation in differentiating cells. In addition to its 'histone deposition' function (Sobel et al., 1995), HDACm might also regulate chromatin remodelling through meiosis (Sommerville et al., 1993). The pool of HDACm stored in the GV and nuclei of the cleavage-stage embryo is not distributed throughout the nucleoplasm or located on the chromosomes but rather is restricted, along with the retinoblastoma-associated protein p48 (RbAp48), to the envelope region of both the GV and embryonic karyomeres (Lemaitre et al., 1998; Ryan et al., 1999). This distribution might serve to prevent premature deacetylation of core histones that are stored in protein aggregates within the nucleoplasm. Both HDACm and RbAp48 can be recovered from GVs in protein complexes of ~300 kDa that were shown to have deacetylase activity. However, activity is abolished by treatment of the complexes with alkaline phosphatase (Ryan et al., 1999). This observation led us to consider the possiblity that at least some of the activities of HDACm are regulated by phosphorylation. HDACm is an orthologue of yeast Rpd3 (Ladomery et al., 1997) and can be grouped with mammalian HDAC1-3 and HDAC-8 as a class 1 enzyme (de Ruijter et al., 2003). Recently, it has been shown that phosphorylation of human HDAC1 by the protein kinase CK2 promotes both enzyme activity and protein complex formation (Pflum et al., 2001). Similar effects of CK2 phosphorylation have also been reported for HDAC2 (Sun et al., 2002; Tsai and Seto, 2002). It is now recognized that CK2 can have a global role in remodelling chromatin (Barz et al., 2003).

Maternally-encoded HDACm, like other class 1 enzymes,

consists of an N-terminal acetyl-metabolizing core and a highly charged C-terminal region postulated to regulate enzyme function (Ladomery et al., 1997). Requirement of the tail domain for import of HDACm into the GV has been tested previously in vivo by injecting radiolabeled fragments into the cytoplasm and recording subsequent levels in isolated GVs. It has been shown that injection of ^{35}S-labeled HACDm protein into the cytoplasm of *Xenopus* oocytes results in a tenfold concentration of the protein in the GV after 24 hours (Ryan et al., 1999). By comparison, a truncated polypeptide (ΔH), which lacks the charged tail domain, fails to be substantially concentrated in the GV (Ryan et al., 1999). The kinetics of import of HDACm are similar to those reported for nucleoplasmin (Vancurova et al., 1995), the efficient transport of which appears to be dependent on phosphorylation by an associated CK2 activity. Here, we show that CK2 phosphorylation of specific sites on HDACm influences not only enzyme activity in vivo, but also translocation to the nucleus by way of the C-tail domain being bound to and released from nuclear import factors. Once in the GV, overexpressed HDACm binds to lampbrush chromosomes leading to chromatin condensation, an activity dependent on the presence of two of the CK2 phosphorylation sites.

Materials and Methods

DNA constructs, mutagenesis and recombinant proteins

The glutathione S-transferase (GST) fusion proteins: GST-ΔV, GST-ΔR and GST-ΔR/ΔH were constructed from cDNA clone *AB21* (EMBL accession number X78454) encoding HDACm (Ladomery et al., 1997). GST-ΔV is an N-terminal deletion of HDACm that removes the enzyme core leaving the C-terminal hydrophilic region fused to GST. It was created by cutting *AB21* DNA with *Pvu*II and ligating, in frame, to a cut pGEX (Pharmacia) vector. GST-ΔR is a fusion protein containing the complete HDACm sequence minus the N-terminal 34 amino acid residues. It was created from an *Eco*R1 fragment of *AB21* DNA. GST-ΔR/ΔV is a fusion protein containing only the enzyme core of HDACm created from an *Eco*R1/*Hin*dIII double digest of *AB21* DNA. All fusion proteins were isolated on glutathione-Sepharose 4B (Pharmacia) according to the manufacturer's instructions. The cDNA fragment encoding the 167 C-terminal residues of HDACm (GST-ΔV) was mutated at putative CK2 phosphorylation sites by two-step PCR through paired oligodeoxyribonucleotides containing single base changes to give serine or threonine to alanine substitutions.

Oocyte extracts

Oocytes were obtained from female *Xenopus laevis*, sorted into stages (Dumont, 1977) and maintained at 22°C in OR-2 medium as described (Peng, 1991). GVs and cytoplasms were isolated under paraffin oil as described (Ryan et al., 1999). Nuclear extracts were made by centrifuging 50 GVs from the oil phase into 50 μl of protein kinase buffer (PKB) (0.1 M KCl, 5 mM $MgCl_2$, 1 mM dithiothreitol, 20 mM Tris-HCl pH 7.5) and freezing at –20°C. After removing the oil from the frozen aqueous phase, the extract was homogenized, mixed with 50 μl of glycerol and kept at –20°C for up to 5 days. CK2 was partially purified from GV extracts by chromatography on heparin-Sepharose (Pharmacia): after binding in 0.1 M KCl buffer and extensive washing with 0.2 to 0.5 M KCl, enzyme activity was eluted in 1 M KCl. Cytoplasmic extracts were made from ten cytoplasms homogenized in 100 μl of PKB and mixed vigorously with an equal volume of 1,1,2-trichlorotrifluoroethane (Sigma). After centrifugation to remove yolk, lipid and pigment with the organic phase, the aqueous layer was further centrifuged at 100,000 ***g*** for 2 hours at 2°C and the supernatant (SN100) was aliquoted and kept at –70°C until use.

Microinjection

Recombinant proteins and IgG fractions (in the range 2-20 ng) were injected into the cytoplasms of stage V oocytes and expression vector DNA (~1 ng) was injected into the GVs of stage IV oocytes. For transcription studies, each oocyte was injected with 0.1 μg of BrUTP (Sigma). To induce maturation, stage VI oocytes were incubated in the presence of 5 nM progesterone. At 2-48 hours, GVs and cytoplasms were isolated under oil.

Protein phosphorylation

Extract from 10 GVs or from an equivalent amount of CK2, or SN100 from two cytoplasms was added to 10 μg of fusion protein (GST-ΔR, GST-ΔR/ΔH or GST-ΔV) bound to 100 μl glutathione-Sepharose 4B. Phosphorylations were carried out in protein kinase buffer by adding 5 μCi of [γ-^{32}P]ATP (3000 Ci/ mmol, Amersham), or ATP to 1 mM, with incubation at 22°C for 30 minutes. After extensive washing of the resin with PKB, phosphorylated protein was eluted with 10% reduced glutathione, 2% n-octyl-β-D-glucopyranoside. Samples were run on SDS-PAGE gels and analysed by autoradiography.

Identification of phosphorylated residues

Phospholabeled GST-ΔV fusion protein was digested with trypsin (20 μg/ml) in 0.1 M ammonium bicarbonate at 37°C for 4 hours. After lyophilization, the sample was raised in 50 μl of 0.1% trifluoroacetic acid and 20 μl of this was applied to a C-18 microbore column. The elution gradient was a 5 minute isocrat step of acetonitrile, followed by a gradual rise to 50% acetonitrile over 30 minutes and a 10 minute rise to 95%. Fractions (80 μl) were collected every minute and 2 μl aliquots were spotted on filter paper and assayed overnight for radioactivity using a phosphorimager. Peak radioactive fractions were lyophilized and resuspended in 10 μl of 30% acetonitrile. These samples were spotted on to a half disk of Sequelon-AA (Millipore) membrane (PVDF derivitised with arylamine groups) and dried at 55°C on a heating block. The dried peptide was then attached to the membrane by adding 5 μl of a 10 mg/ml solution of carbodiimide. After leaving it at room temperature for 20 minutes, the membrane was washed three times in 0.5 ml of 50% methanol and placed in the sequencer. The extracted ATZ derivative from each sequencing-cycle was collected, dried and resuspended in 10 μl of 90% methanol. Aliquots of 2 μl were collected on filter papers and assayed for radioactivity using a phosphorimager.

Immunostaining

Total protein minus pigment and yolk, equivalent to four GVs or one cytoplasm, was separated by SDS-PAGE and transferred to nitrocellulose membranes (Schleicher and Schuell). Protein transfers were developed using enhanced chemiluminescence (ECL) (Amersham) after reaction with anti-GST (1:10,000) (Sigma), anti-Cpep (1:5000) or anti-importin-α (1:5000) and peroxidase-conjugated anti-mouse IgG or anti-rabbit IgG (1:20,000) (both Sigma). ECL films and autoradiographs were scanned and analysed with Gene Tools Gel software (Syngene). Lampbrush chromosomes were immunostained as described (Sommerville et al., 1993).

In vitro protein binding

GST fusion proteins (phosphorylized and not phosphorylized) were immobilized on glutathione-Sepharose 4B at ~1 μg protein per 5μl beads and treated with CK2 with or without ATP as described above.

After washing with binding buffer (BB) (0.1 M NaCl, 10 mM $MgCl_2$, 2 mM dithiothreitol, 20 mM Tris-HCl pH 7.5), the protein beads were incubated with soluble extract from two cytoplasms (SN100) or 10 GVs in PKB at 22°C for 10 minutes. Unbound material was retained and precipitated with 3 volumes acetone, the beads were washed 4 times with 10 volumes BB and bound material was eluted with 10% reduced glutathione, 2% *n*-octyl-β-D-glucopyranoside or SDS-PAGE sample buffer (Sigma). Recombinant importin-α (Calbiochem) was immobilized on nitrocellulose by absorbing 0.1 μg of protein onto 5 mm^2 membrane followed by blocking with 10% milk in BB at 22°C for 20 minutes. The importin-α membrane squares were rinsed in BB and incubated with GST fusion proteins, 0.1 μg in 20 μl BB, at 22°C for 20 minutes. Some fusion protein samples were pre-phosphorylated, as described above, before binding to filters. Post-phosphorylation involved incubation of the filters with GV extract (10 GVs plus 1 mM ATP in 12 μl PKB) at 22°C for 20 minutes. Released protein was collected, filters were washed with BB and retained protein was eluted with SDS-PAGE sample buffer.

Results

The charged tail domain is phosphorylated at selected sites by nuclear protein kinase CK2

One feature of HDACm, also found in its class 1 orthologues (Ladomery et al., 1997), is the presence of the charged C-terminal domain, which in the *Xenopus* protein contains 35% acidic (D+E) residues and 23% basic (K+R) residues (Fig. 1A). It is noted that, within this domain, HDACm contains a sequence similar to the bipartite nuclear localization signal (NLS) (Dingwall and Laskey, 1991), which is contained in the *Xenopus* nuclear protein N1/N2 (Fig. 1B). This sequence similarity might have biological significance because the two proteins have related functions: whereas HDACm deacetylates histones H3 and H4, N1/N2 acts as a chaperone for

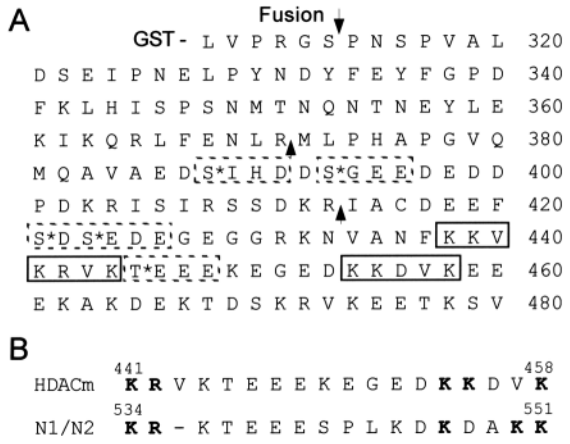

Fig. 1. Sequence motifs present in the charged C-terminal domain of HDACm. (A) DNA encoding the C-terminal 167 amino acid residues of HDACm was expressed as a fusion protein with glutathionine S-transferase (GST-ΔV). The fusion site is indicated by an arrow and trypsin sensitive sites are indicated by arrowheads. Potential CK2 phosphorylation sites are boxed by dashed lines, with the phosphorylated residue indicated by an asterisk. Groups of basic (K+R) residues, which might contribute to a nuclear import signal (NLS), are boxed by solid lines. (B) The proposed bipartite NLS of HDACm is aligned with the reported NLS of the histone H3/H4 chaperone N1/N2. Numbers indicate the residue positions in the protein sequences.

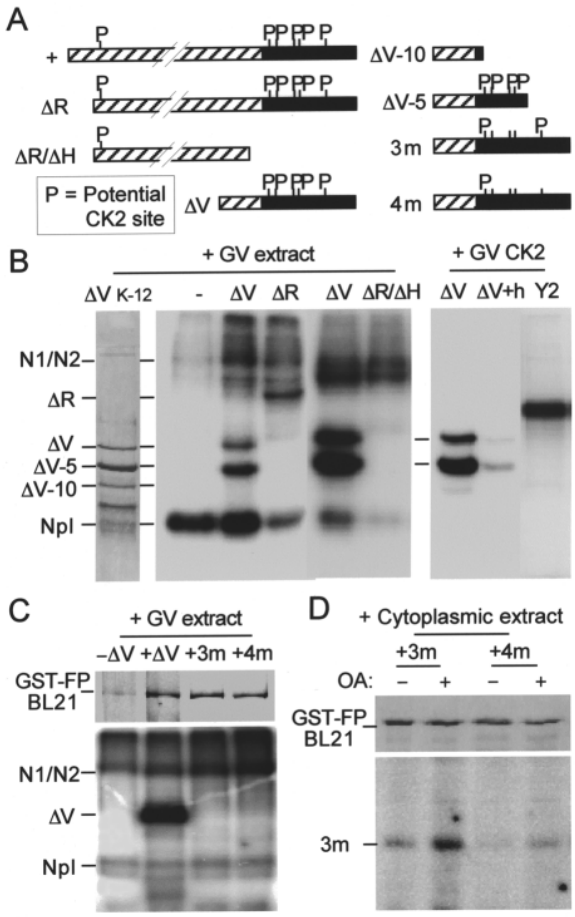

Fig. 2. Phosphorylation of fusion proteins that contain different regions of HDACm by CK2 activity extracted from oocytes. (A) Diagram showing the relative positions of potential CK2 phosphorylation sites (P) within the complete HDACm protein (+) and various deletions and mutations. The enzymatic core site is hatched and the C-terminal hydrophilic region is black. All six sites are contained in the GST-ΔR deletion, the five sites present in the hydrophilic region are deleted in GST-ΔR/ΔH and the single N-terminal site is deleted from GST-ΔV. Deletion of ~10 kDa from the C-terminus removes all five of the marked sites in the hydrophylic region, whereas deletion of ~5 kDa removes only the most C-terminal site. In the GST-ΔV mutant 3m, the three sites most towards the center are mutated (Ser to Ala) and in the mutant 4m the most C-terminal site is also mutated (Thr to Ala). (B) Phosphorylation of GST-fusion proteins expressed in a K12 strain of *E. coli*. The stained gel (left) shows that partial hydrolysis of GST-ΔV generates fragments that have lost a molecular mass of ~5 kDa, ~10 kDa and ~15 kDa from the C-terminus. Abundant proteins from an added nuclear extract (GV), N1/N2 and nucleoplasmin (Npl) are also seen as stained bands. Phospholabeling with ^{32}PγATP by a GV extract (middle) shows that labeling is restricted to the hydrophobic region but is excluded from the C-terminal ~10 kDa. Phospholabeling of GST-ΔV by CK2 isolated from GVs (right) removes labeling due to N1/N2 and nucleoplasmin and is almost completely sensitive to 10 μg/ml heparin. The known CK2 substrate *Xenopus* FRGY2 (Y2) is shown as a positive control. (C) Phosphorylation of GST-ΔV and 3m and 4m mutants expressed in a BL21 strain of *E. coli* by oocyte nuclear (GV) and cytoplasmic extracts (D). Whereas GV extract labels neither 3m nor 4m (C), a small, but significant, labeling of 3m is detected with cytoplasmic extract in the presence of 10 nM okadaic acid (OA, D). The stained gels (top of each panel) indicates equal loading of GST-fusion proteins (GST-FP).

diacetylated H3 and H4 awaiting incorporation into chromatin (Dilworth et al., 1987; Kleinschmidt and Seiter, 1988).

In addition to its putative NLS, HDACm contains six possible sites for phosphorylation by CK2 but no obvious sites for phosphorylation by cell-cycle-dependent kinases. Five of the six CK2 sites are located in the charged tail domain and are represented in GST fusion proteins as shown in Fig. 2A. CK2 activity is readily available from GVs isolated under oil and this activity can be separated from most of the nuclear protein by affinity-binding to heparin-Sepharose. Nevertheless, the presence of nuclear proteins provides internal markers for the phosphorylation reactions: the histone H3/H4 chaperone N1/N2 (110/105 kDa on SDS-PAGE) and the histone H2A/H2B chaperone nucleoplasmin (30 kDa on SDS-PAGE). Incubation of the different fusion proteins (Fig. 2A) with GV extract and [γ-^{32}P]ATP shows that only proteins containing the charged tail domain (ΔR and ΔV) are phospholabeled, whereas proteins containing only the N-terminal CK2 site are never phospholabeled (Fig. 2B). The protein undergoes limited proteolysis when expressed in *Escherichia coli* K-12 strains, resulting in products running on SDS-PAGE with apparent masses of 43 kDa and 38 kDa because of polypeptide cleaved from the carboxyl end. Because the 43 kDa product phosphorylates almost as efficiently as complete GST-ΔV, we conclude that accessible sites are located beyond 5 kDa from the C-terminus. However, the 38 kDa product is not phospholabeled, indicating lack of availability of sites located beyond 10 kDa from the C-terminus. Little difference is seen in phospholabeling patterns of the GST fusion proteins using either GVs or isolated CK2 (Fig. 2B), indicating that the activity of CK2 is sufficient to account for the phosphorylation of HDACm by GVs. As predicted, the CK2 activity is inhibited by low concentrations of heparin and is also specific for the mRNA-binding proteins FRGY2a/b (Fig. 2B).

The phospholabeled sites were identified by analysing peptides, produced by trypsin digestion of full-length phospholabeled GST-ΔV, on an amino acid sequencer. Two peaks of radioactivity were obtained by separation of the digest on fine-bore HPLC (Fig. 3A). Peptides from the peak fractions were then sequenced and material from each cycle was collected on filters and assayed for radioactivity. In peptide 1 (Fig. 3B), peaks of radioactivity were recovered from cycles eight and ten, corresponding to the two serine residues present at these positions. These same peaks of radioactivity were found in two separate sequencing runs. In peptide 2 (Fig. 3C), radioactivity was recovered only in cycle 22, indicating that the serine residue at position 22 but not the serine residue at position 17 (which is another of the potential CK2 sites), is phosphorylated. No evidence was found of a peptide containing the sequence TEEE in a labeled form, which indicates that the site located within the putative NLS (Fig. 1B) is not a target of nuclear CK2. From these results, it appears that phosphorylation of HDACm by nuclear CK2 in vitro is restricted to three out of six possible sites.

Point mutations block in vitro phosphorylation

In accord with the detection of three phospholabeled residues by sequencing, the point mutations S393A, S421A and S423A together (3m) were found to be sufficient to prevent any phospholabeling of GST-ΔV by nuclear CK2 (Fig. 2C). In these, and most subsequent experiments, the fusion proteins were recovered from *E. coli* BL21 strains and showed no sign of proteolysis. The mutation T445A was added to make a 4m version, but the lack of any phospholabeling in both 3m and 4m confirmed that the nuclear CK2 activity had no effect on the T445 site in vitro. However, a transient phospholabeling of T445 was detected by using oocyte cytoplasmic SN100 as a source of protein kinase activity. In the presence of the phosphatase inhibitor okadaic acid the 3m mutant showed labeling significantly above the 4m (background) level (Fig. 2D), indicating that T445 might be phosphorylated in the cytoplasm.

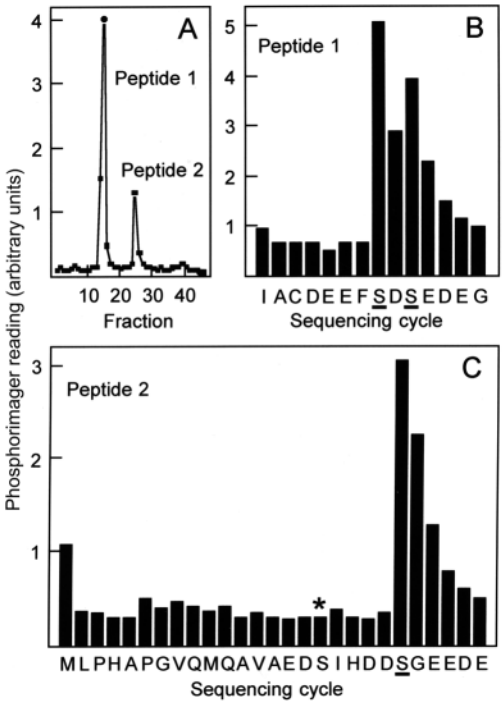

Fig. 3. Mapping of phosphorylation sites in HDACm. GST-ΔV was phospholabeled in vitro using oocyte nuclear CK2. (A) Only two phospholabeled tryptic peptides (1 and 2) were recovered by HPLC. (B) Sequencing of peptide 1 reveals two phospholabeled residues at positions S421 and S423. (C) Sequencing of peptide 2 reveals a single phospholabeled residue at positions S393. The potential site S388 (asterisk) is not labeled.

Nuclear uptake is dependent on the C-terminal region containing the putative NLS

On injecting phospholabeled GST-ΔV into the cytoplasm of stage V oocytes, the kinetics of nuclear uptake can be recorded by SDS-PAGE autoradiography of the contents of GVs isolated after various time intervals. From the partially proteolysed GST-ΔV sample injected, only the protein with a complete C-terminus is accumulated in the GV (Fig. 4A). The 42 kDa (ΔV-5) truncated form is not detected in the GV and is eventually (>50 hours) dephosphorylated and/or degraded in the cytoplasm. The kinetics of nuclear uptake of GST-ΔV (Fig. 4B) show a rapid and efficient translocation: about 80% of the protein is isolated with the GV at 8 hours after injection. This is much quicker than seen on injecting full-length HDACm,

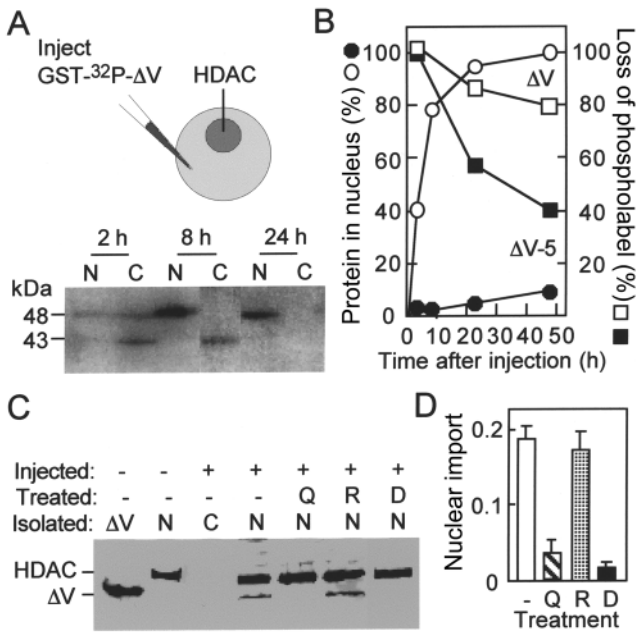

Fig. 4. Both the C-terminal region of HDACm and phosphorylation are required for nuclear uptake. (A) Phospholabeled GST-ΔV (10 ng) was injected into the cytoplasm of stage V oocytes and incorporation of label into the GV was monitored from isolated nuclei and cytoplasms. Whereas most of the full-length fusion protein was imported within 8 hours, the GST-ΔV-5 degradation product remained in the cytoplasm, again indicating that the C-terminal ~5 kDa region is required for nuclear import. (B) Quantitation of the amounts and distribution of GST-ΔV and GST-ΔV-5 in GVs and cytoplasms up to 48 hours post-injection not only confirms the requirement for the C-terminal ~5 kDa region but also indicates that it is required for stability of the protein. (C) The requirement of phosphorylation for nuclear import of GST-ΔV is shown by comparing the amounts of fusion protein present in GVs at 24 hours post-injection with the amount of endogenous nuclear HDACm. Import is severely restricted in the presence of the inhibitors of CK2 activity, quercetin (Q, 60 nM) and 5,6-dichloro-1β-D-ribofuranosylbenzimidazole (D, 50 μM), whereas the inactive analogue of quercetin, 3β-D-rutinoside (R, 60 nM), has little inhibitory effect. Immunoblot using antibody directed against the C-terminal peptide of HDACm. (D) Quantitation of three repeat experiments confirm the requirement of phosphoryation for efficient nuclear import of GST-ΔV. Density scan of each GST-ΔV band is expressed as a fraction of the density scan of the corresponding endogenous HDACm band.

indicating that the enzyme core might interact with, and that its import might be restricted by, cytoplasmic proteins. Passive diffusion of GST-ΔV into the GV is unlikely because the truncated version ΔV-5 remains largely in the cytoplasm. Protein import in these experiments amounts to more than 1 ng/hour/oocyte over the first few hours, which compares with the rate of synthesis (and presumably the rate of nuclear translocation) of core histones in full-grown oocytes (40 pg/hour) (Adamson and Woodland, 1974).

Inhibition of CK2 activity blocks nuclear uptake of the tail domain

Injection of GST-ΔV into the cytoplasm of oocytes treated with the inhibitor of CK2, quercetin, its inactive analogue quercetin 3β-D-rutinoside (rutin) and with the inhibitor 5,6-dichlor-1β-D-ribofuranosylbenzimidazole (DRB), indicates that phosphorylation is required for nuclear import (Fig. 4C). The amount of GST-ΔV imported after 18 hours was compared with the amount of endogenous HDACm, both detected by antibodies raised against the C-terminal 17 residues of HDACm (Fig. 1A) (Ryan et al., 1999). Quantitation of band intensities from three separate injection experiments shows that inhibition of protein kinase activity by quercetin and DRB greatly reduces nuclear import of GST-ΔV (Fig. 4D). However, these results do not identify GST-ΔV as the prime target for phosphorylation-dependent import. Identification of crucial targets is better achieved by site-specific mutagenesis.

Mutation of specific phosphorylation sites alters the efficiency of nuclear import

The rate of nuclear import of mutated proteins was compared with that of non-mutated GST-ΔV by injecting the proteins into the cytoplasm of oocytes, isolating GVs and cytoplasms and immunoblotting the extracts with anti-GST. In addition, recombinant import receptor importin-α was co-injected with the fusion proteins. The efficiency of import of GST-ΔV was markedly improved by co-injecting equimolar amounts of importin-α, whereas mutation of all four of the identified phosphorylation sites (4m), which resulted in poor efficiency of import, was not improved by co-injecting importin-α (Fig. 5A,B). However, mutation of the three sites excepting T445 (3m) actually increased import efficiency over wild type, to an extent which was not improved by co-injecting extra importin-α (Fig. 5A,C). The mutation T445A was sufficient for the substantial decrease in import efficiency seen with 4m, T445A again showing no improvement on co-injecting extra importin-α (Fig. 5A,C). As noted earlier (Fig. 4B), the initial kinetics of nuclear import of GST-ΔV are rapid, at >1 ng/hour/oocyte. That import was not a function of the relatively small mass of GST-ΔV was confirmed by measuring the nuclear co-translocation of anti-GST. Whereas injection of GST-ΔV and 3m resulted in translocation of a substantial amount of co-injected anti-GST to the GV, injection of the T445A mutant translocated much less anti-GST (Fig. 5D). Again, import appeared to be more efficient with 3m than with GST-ΔV. It was concluded that T445 was the potential phosphorylation site that had the most positive influence on efficient nuclear import of GST-ΔV.

Because dissociation of nuclear import complexes is regulated by the small Ras-like GTPase Ran, the effect of co-injecting Ran with GST-ΔV was also checked. Although equimolar amounts of recombinant Ran had little effect on the import kinetics of GST-ΔV, co-injection of the mutant RanQ69L, which is defective in GTPase activity and inhibits NLS-dependent protein import in *Xenopus* oocytes (Izaurralde *et al.*, 1997), significantly inhibits the initial rate of GST-ΔV import (Fig. 5E,F), thus implicating Ran in the import process.

Phosphorylation of S421 and S423 enhances the release of GST-ΔV from importin-α

To examine the role of phosphorylation of GST-ΔV on its binding to, and release from, import receptors, in vitro binding

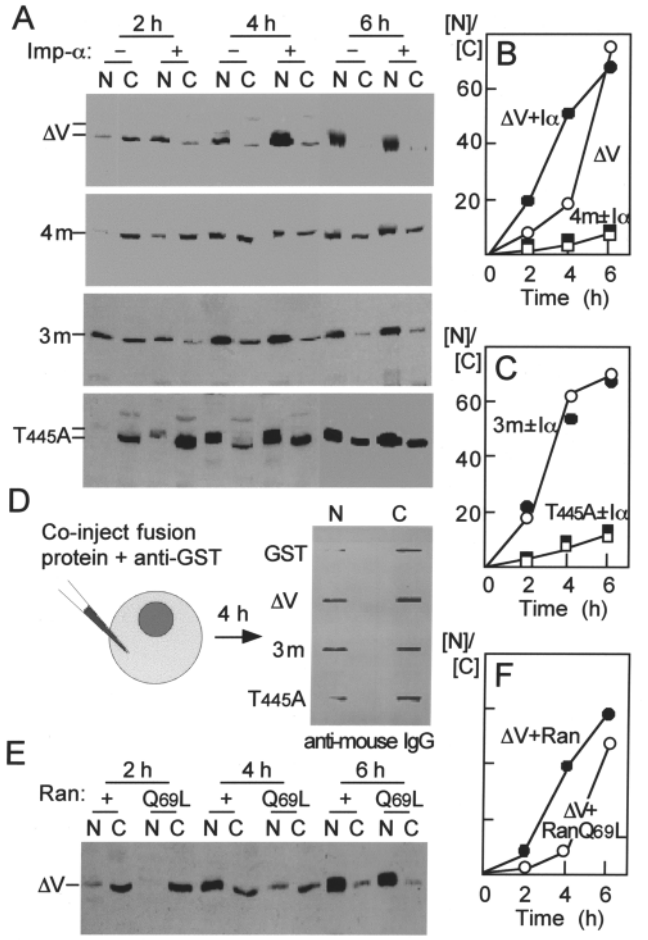

Fig. 5. Identification of phosphorylation sites required for efficient nuclear import of GST-ΔV in vivo. (A) 10 ng of GST-ΔV or mutants: 4m (S393A, S421A, S423A, T445A); 3m (S393A, S421A, S423A); and T445A alone, were injected into the cytoplasm of oocytes, with and without co-injection of 12 ng of importin-α, and GVs and cytoplasms were recovered after 2, 4 and 6 hours. Extracted protein was immunoblotted using antibody directed against the C-terminal peptide of HDACm. (B) Quantitation of results from upper two panels of (A) normalized to ratios of nuclear:cytoplasmic concentration. GST-ΔV plus importin-α (filled circles), GST-ΔV minus importin-α (open circles); 4m plus importin-α (filled squares), 4m minus importin-α (open squares). (C) Quantitation of results from lower two panels of (A). 3m plus importin-α (filled circles), 3m minus importin-α (open circles); T445A plus importin-α (filled squares), T445A minus importin-α (open squares). (D) Nuclear import of anti-GST IgG on co-injection with GST, GST-ΔV, 3m and T445A. GVs and cytoplasms were isolated after 4 hours and a slot blot of protein was developed using anti-mouse IgG. (E) Nuclear import of GST-ΔV on co-injection of 5 ng of Ran or of the Ran mutant Q69L. (F) Quantitation of results from (E) showing GST-ΔV plus Ran (filled circles), GST-ΔV plus RanQ69L (open circles).

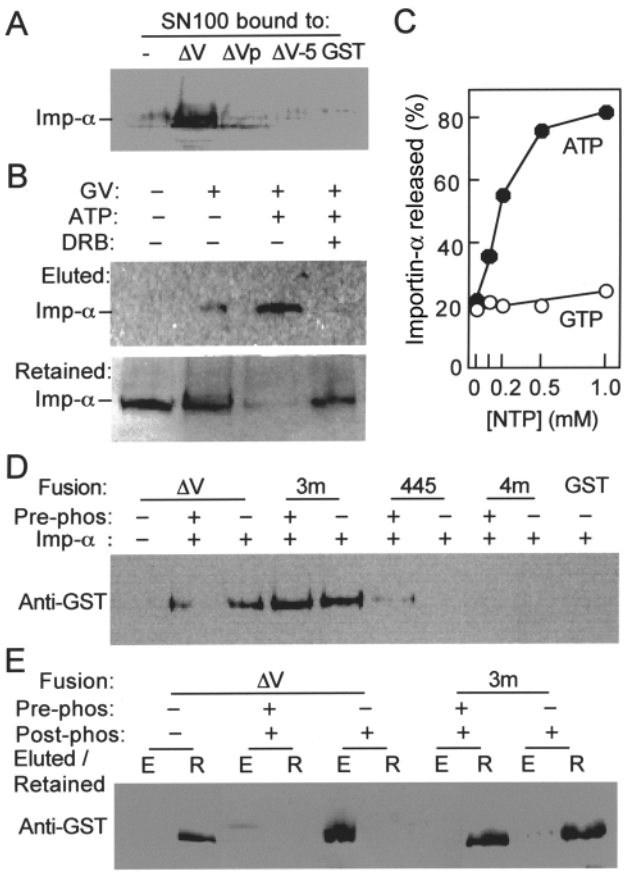

Fig. 6. Interaction of GST-ΔV with importin-α in vitro is influenced by the presence of C-terminal phosphorylation sites. (A) Binding of endogenous importin-α from an oocyte SN100 fraction to GST-ΔV, pre-phosphorylated GST-ΔV (ΔVp), GST-ΔV with deletion of the C-terminal ~5 kDa (ΔV-5) and GST, all immobilized on glutathione-Sepharose. Immunoblot using anti-importin α. (B) Elution of importin-α from immobilized GST-ΔV in the presence and absence of *Xenopus* GV extract, 1 mM ATP and DRB. Importin-α was first bound as in A, track 2. (C) Dependence of release of importin-α from immobilized GST-ΔV by addition of ATP (filled circles) rather than GTP (open circles). As in B, track 3, but with different concentrations of ATP or GTP. Immunoblots were scanned and relative intensities of signal from the importin-α bands were calculated and plotted as a percentage of input protein released. (D) Binding of pre-phosphorylated and non-phosphorylated GST-ΔV, 3m, T445A, 4m and of GST to importin-α immobilized on nitrocellulose filters. Immunoblot using anti-GST. (E) Release of pre-phosphorylated and non-phosphorylated GST-ΔV and 3m from immobilized importin-α after treatment of filters with GV extract plus ATP. Protein eluted (E) and retained (R) was detected using anti-GST.

studies were undertaken using the GST-ΔV mutants. GST-ΔV immobilized on glutathione-Sepharose, specifically binds a small subset of proteins from cytoplasmic SN100 (not shown). A component of 60 kDa was identified by immunoblotting, as importin α (Fig. 6A). Whereas GST-ΔV bound endogenous importin-α, GST-ΔV pre-phosphorylated with nuclear CK2 bound only poorly: GST-ΔV lacking the terminal ~5 kDa failed to bind out any importin-α, as did the GST control (Fig. 6A). Separate additions of GV extract and ATP were required to release importin-α from immobilized GST-ΔV; release was prevented by adding DRB, the inhibitor of CK2 (Fig. 6B). The nucleotide triphosphate required to prevent binding is ATP and not GTP (Fig. 6C), making it unlikely that release was exclusively owing to the import release factor RanGTP, which is present in the GV extract. Further experiments were carried out by immobilizing recombinant importin-α and examining binding and release of the GST-ΔV point mutants. Only non-

phosphorylated GST-ΔV bound importin-α, whereas both phosphorylated and non-phosphorylated 3m mutants bound it effectively; phosphorylated GST-ΔV, phosphorylated and non-phosphorylated mutants T445A, 4m and control GST all bound importin-α only poorly (Fig. 6D). However, of the bound forms, only non-phosphorylated GST-ΔV was released from immobilized importin-α by post-incubation with GV extract plus ATP, most of the 3m mutant were retained after similar treatment (Fig. 6E). The small amount of bound GST-ΔV from the pre-phosphorylated sample (Fig. 6D, track 2) was also released after post-incubation (a faint band was seen in Fig. 6E, track 3). These results, and further experiments (not shown) with a 2m mutant form (S421A and S423A), indicate that the phosphorylatable residues S421 and S423 are required for effective release of GST-ΔV from importin-α in vitro.

Nuclear HDACm is dephosphorylated during progesterone-induced oocyte maturation

On closer examination of the immunobots of GST-ΔV imported into the GV, we noticed that the immunoreactive region is composed of several closely-arrayed sub-bands. Whereas the single mutation T445A resulted in the loss of the isoform with the least mobility, the triple mutation 3m showed a single band (Fig. 7A).

On western blots, endogenous HDACm isolated from GVs of stage VI oocytes also shows multiple bands. At least four distinct isoforms can be discriminated (Fig. 7B) and it is reasonable to assume that they correspond to non-phosphorylated HDACm and to the one phosphorylated at one, two and three of the sites already described. However, this profile of multiple isoforms undergoes changes within the first few hours of treating the oocytes with progesterone. Progesterone induces oocyte maturation, which is characterized by many changes including chromatin condensation, hyper-phosphorylation of lamins and GV breakdown (GVB). However, in the few hours preceding GVB, intact GVs can still be isolated and immunoblotting of their proteins shows a time-dependent resolution of multiple HDACm bands into the single, fastest migrating, band. Probably, this change is because of the activation of a nuclear phosphatase. Indeed, treatment of zero time extracts with alkaline phosphatase also results in the visualisation of the immunostaining material to a single, sharp band (Fig. 7B). Therefore, we can see changes in the phosphorylated status of endogenous HDACm which can be related to the effects that we have described with recombinant GST-ΔV when examined both in vivo and in vitro.

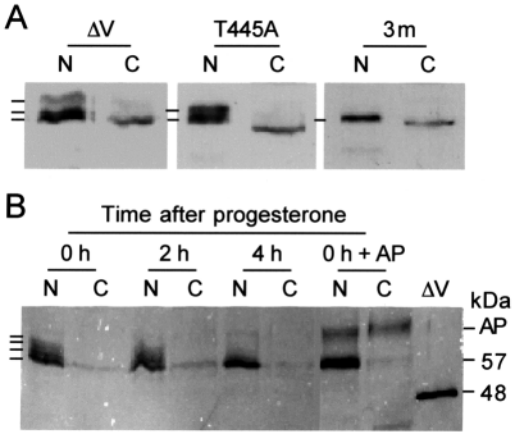

Fig. 7. Phosphorylated isoforms of both GST-ΔV and endogenous HDACm can be detected in GVs. (A) Immunoblots of GST-ΔV, T445A and 3m from GVs and cytoplasms isolated at 4 hours post-injection into the cytoplasm. Bars on the left indicate the positions of three possible isoforms. (B) Dephosphorylation of nuclear HDACm in vivo during oocyte maturation. Stage VI oocytes were treated with 0.5 μM progesterone to induce maturation and GVs and cytoplasms were isolated at 0, 2 and 4 hours. Samples taken at 4 hours post-hormone were also treated with 2 units/μl of alkaline phosphatase. Immunoblot using antibody directed against the C-terminal peptide of HDACm. GST-ΔV is shown as a non-phosphorylated control for antibody detection. Bars on the left indicate the positions of four possible isoforms, the fastest migrating of which corresponds to non-phosphorylated HDACm at 57 kDa.

Mutation of S421A and S423A negates the activity of over-expressed HDACm in condensing endogenous chromatin

We showed previously that over-expression of HDACm can lead to changes in the endogenous chromatin: the transcribing loops retract and the chromosomes shorten and condense (Ryan et al., 1999). In the experiments described here, eight out of ten complete karyotypes examined from HDACm-injected oocytes showed chromosome shortening of >40% compared with homologues from non-injected oocytes. Chromatin condensation (Fig. 8B,E) is associated with loss of incorporation of BrUTP (Fig. 8C) and loss of immunoreactivity with antibody that detects acetylated histone H4 (Fig. 8D). In addition, antibody against HDACm labels the chromosomes less extensively, the reaction being restricted to the dense chromomeric axis (Fig. 8A). However, on over-expression of the double mutant, S421A/S423A (HDACm-2m), chromosome morphology remains normal Fig. 8G,J), the loops incorporate BrUTP (Fig. 8H), antibody to acetylated histone reacts intensely with the chromomeric axis (Fig. 8I) and antibody to HDACm reacts more extensively with chromeres and loops (Fig. 8F). Thus the normal nuclear function of HDACm, in deacetylating histones leading to loss of transcriptional activity and chromatin condensation, appears to be disrupted by mutation of the two major phosphorylation sites.

Discussion

Nuclear import and phosphorylation

Import of a protein into the nucleus is generally dependent upon the presence of a nuclear localization signal. The NLS can take the form of either a block of mainly basic residues, [the model sequence is 126PKKKRVK132, occurring in simian virus 40 (SV40) large T antigen (T-ag)] or a bipartite motif in which two short basic regions are separated by ten unspecified residues (Dingwall and Laskey, 1991). The function of the NLS can be regulated, however, by phosphorylation of proximal sites, resulting in either acceleration or inhibition of nuclear uptake of the protein. For instance, the rate of NLS-dependent nuclear import of T-ag is increased 40-fold by phosphorylation of S112 by CK2,

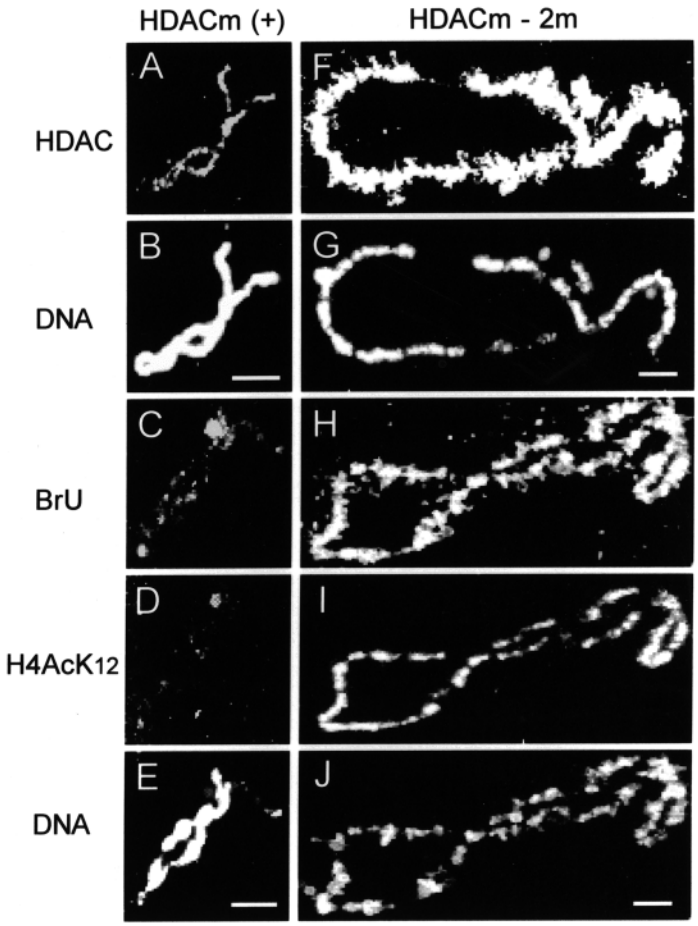

Fig. 8. Effects of overexpression of HDACm and HDACm-2m on the endogenous chromatin of *Xenopus* oocytes. Vector expressing HDACm (+) or HDACm-2m (S421A, S423A) was injected into GVs of stage IV oocytes and after 24 hours nuclear spreads were made to view lampbrush chromosomes. Some oocytes were co-injected with 50 ng of bromo-UTP to detect endogenous RNA transcription. Chromosomes were immunostained using antibodies against HDACm (A,F), incorporated bromouridine (BrU) (C,H) and histone H4 acetylated at residue lysine12 (H4AcK12) (D,I). All preparations were counterstained with 4,6-diamidino-2-phenylindole (DAPI) to detect chromosomal DNA (B,E,G,J). Bars, 20 μm.

whereas phosphorylation of T124 by cdc2 inhibits nuclear import (Rhis et al., 1991; Jans et al., 2000). Phosphorylation of such residues in the vicinity of the NLS acts to regulate import through the modulation of protein-protein interactions.

The microinjection experiments in this report show that the C-terminal region of ~40 amino acid residues is essential for the efficient nuclear uptake of HDACm (Fig. 4). Within this region, we tentatively identify the sequence 438**KK**V**KR**V**K**TEEEKEGED**KK**DV**K**458 as being important for nuclear uptake. Either the first seven residues, or a bipartite grouping of residues 441-442 and 454-458 could act as an NLS. Interestingly, a similar sequence 531LV**RKKRK**TEEESPLKD**K**DA**KK**551 was identified as the NLS in the *Xenopus* nuclear protein N1/N2, originally as the first seven residues (Kleinschmidt and Seiter, 1988) and latterly as a bipartite grouping of residues 534-535 and 545-549 (Dingwall and Laskey, 1991). HDACm and N1/N2 have related functions in the utilization of histones during the early development of *Xenopus*. During oogenesis, there is accumulation of a large pool of core histones (84 ng/cell) (Adamson and Woodland, 1974) sufficient for assembly of much of the new chromatin through the 12 rapid cell divisions of early embryogenesis. The stored histones exist in oocytes in association with specific protein chaperones, which together form soluble complexes: histone H3/H4 coupled with N1/N2 to form a complex sedimenting at 5S and histone H2A/H2B coupled with nucleoplasmin to form a complex sedimenting at 7S (Kleinschmidt et al., 1985). However, these stored core histones are accumulated as acetylated forms. Non-nucleosomal histone H4, for example, was shown to be diacetylated, not only in *Xenopus* oocytes and early embryos (Almouzni et al., 1994), but also during the early development of sea urchins (Chambers and Shaw, 1987) and starfish (Ikegami et al., 1993). Once the acetylated histones are incorporated into chromatin, the new nucleosomal structures are stabilized by histone deacetylation (Wolffe, 1994). HDACm is believed to be the catalytic agent involved in developmentally-regulated deacetylation in *Xenopus* (Ladomery et al., 1997). Histone deacetylase activity is the property of a 300 kDa protein complex containing HDACm and RbAp48/46 that has been shown to deacetylate peptides representing the N-terminal region of histone H4, in addition to mixtures of acetylated core histones (Ryan et al., 1999). The HDACm complex and N1/N2 similarly interact with core histones in the nucleus and so might be expected to share regulatory features.

Nuclear import of the other chaperone of histone H2A/H2B, nucleoplasmin, has been shown to be regulated by phosphorylation, particularly phosphorylation of sites in the vicinity of the NLS by CK2 (Vacurova et al., 1995). Of the six potential sites in HDACm for phosphorylation by CK2, we show here (Figs 2, 3) that three are phosphorylated in vitro by a form of CK2 isolated from *Xenopus* GVs. These three sites are occupied by serine residues within the charged tail domain, at positions 15, 17 and 45 upstream of the start of the putative NLS. The most proximal two sites are more efficiently phosphorylated than the distal site and their location, relative to the putative NLS, is similar to the CK2 sites (at positions 14 and 15) whose phosphorylation enhances the rate of nuclear import of SV40 T-ag (Rhis et al., 1991; Jans et al., 2000). By comparison, the CK2 sites in nucleoplasmin, which are most probably used in NLS-dependent regulation, are located at positions 7 and 8 downstream the end of the NLS (Vacurova et al., 1995). However, we show here that mutation of the three upstream sites at position 45, 17 and 15 relative to the putative NLS (S393A, S421A and S423A) had no negative effect on nuclear import of the C-tail domain of *Xenopus* HDACm, when fused to glutathione S-transferase (GST-ΔV; Fig. 5).

A fourth potential CK2 site in GST-ΔV that is not phospholabeled by nuclear CK2, but is weakly phosphorylated by cytoplasmic extracts in the presence of phosphatase inhibitor (Fig. 2D) is 445TEEE448, which lies within the putative bipartite NLS. This same sequence occupies an identical position within the bipartite NLS of N1/N2. Mutation of T445A at this site had the greatest effect of all point mutations studied in the import of GST-ΔV, resulting in an ~fivefold reduction in its rate of translocation into the GV (Fig.

5). Thus, in *Xenopus* HDACm, phosphorylation of a site within the NLS, rather than of proximal sites outside the NLS, might regulate its rate of nuclear uptake.

The responsible cytoplasmic protein kinase has not been completely characterized, but its activity is inhibited by the same agents that inhibit nuclear CK2 (not shown) and the target sequence 445TEEE448 represents a potential CK2 site. Selection of only one of the four potential CK2 sites for cytoplasmic phosphorylation could be owing to protein masking of the other three sites or to a special organization of the CK2 itself. For instance, the cytoplasmic CK2 that phosphorylates oocyte mRNP particles lacks a conventional β regulatory subunit (A.J.L. and J.S., unpublished).

Interaction of the tail domain of HDACm with importin-α

If the NLS of HDACm has a bipartite configuration, it should be recognized first by the transport factor importin-α (Kuersten et al., 2001; Weis, 2002). In the nuclear import studies reported here, it was found that co-injection of equimolar amounts of recombinant importin-α into the cytoplasm of oocytes resulted in a significant increase in the rate of nuclear import of GST-ΔV (Fig. 5). Because excess amounts of importin-α are present in oocytes (Izaurralde et al., 1997), this effect might be because premixing of GST-ΔV and importin-α favors complex formation before injection. However, an increase in the import rate was not seen with the 3m mutant (S393A, S421A and S423A), implying that phosphorylation of these sites has no effect on the ability of importin-α to recognize the NLS of HDACm. Also, the failure of the single mutant T445A to be imported was not reversed by co-injection with equimolar amounts of importin-α. Therefore, only availability of the phosphorylation site T445 was identified as a requirement for efficient import of HDACm.

Molecular interaction of GST-ΔV with importin-α was confirmed in affinity binding studies. Whereas immobilized non-phosphorylated GST-ΔV was shown to bind out importin-α from cytoplasmic SN100, pre-phosphorylation of GST-ΔV with nuclear CK2 inhibited this interaction (Fig. 6A-C). That phosphorylation of those sites most sensitive to nuclear CK2 (S421 and S423) triggers release of GST-ΔV from importin-α, was demonstrated by the binding and elution profiles of mutant forms from immobilized recombinant importin-α (Fig. 6D,E).

Because the small Ras-related GTPase Ran is required for the dissociation of imported complexes (Kuersten et al., 2001; Weis, 2002), the contributions of CK2 phosphorylation and RanGTP in dissociating the HDACm/importin complex should be considered. Ran is present in oocytes at a concentration of 10 μM (Izaurralde et al., 1997) and is therefore unlikely to be the limiting factor in the microinjection of ~10 ng of GST-ΔV (final concentration of ~0.2 μM) used here. The results, showing no apparent increase in import rate when co-injecting 5 ng (~0.2 μM) of recombinant Ran (Fig. 5F), were therefore expected. However, cytoplasmic co-injection of 5 ng of the Q69L Ran mutant, which has previously been shown to cause premature disassembly of import complexes (Izaurralde et al., 1997), apparently acts as a dominant negative factor, sufficient to suppress the initial rate of import from the injection site (Fig. 5F). Immobilized GST-ΔV effectively binds importin-α in cytoplasmic extracts that contain RanGDP rather than RanGTP and have the potential of phosphorylating T445, although GST-ΔV pre-phosphorylated (primarily at S421 and S423) with nuclear CK2 fails to bind importin-α under the same conditions (Fig. 6A). RanGTP is also unlikely to be the limiting factor in the in vitro release experiments which utilize GV extract that also contains excess GTP and the nucleotide exchange factor RCC1 (Izaurralde et al., 1997). However, release is prevented in the presence of CK2 inhibitor (Fig. 6B) or on using GST-ΔV mutated at S393A, S421A and S423A (Fig. 6E). Therefore, in the presence of nuclear extract containing excess RanGTP, it is CK2 activity and the presence of S393, S421 and S423 (Fig. 6D,E) which makes a critical difference between the ability and failure of the ΔV fragment to be released from the import complex.

Taken together, these results indicate that HDACm is imported into the GV of *Xenopus* oocytes by the binding of importin-α to the bipartite NLS, with the cytoplasmic phosphorylation of T445 within the NLS acting as a possible regulatory factor, and that HDACm is released from the import complex by RanGTP, the nuclear phosphorylation of S421 and S423 promoting this step.

Phosphorylation of HDACm in vivo and its enzyme activity

That the phosphorylation of HDACm is actually occurring in vivo during its import into GVs, is indicated by the separation into multiple immunostaining bands on SDS-PAGE. The multiple banding is seen in protein samples taken from isolated GVs, but not from isolated cytoplasms (Ryan et al., 1999) and we show here that at least four components can be resolved to a single band after treatment with alkaline phosphatase (Fig. 7B). Although the number of slower migrating bands corresponds to the number of phospholabeled residues detected after in vitro phosphorylation, we do not know whether the same sites are used in vivo. In the GVs of full-grown (stage VI) oocytes, the presence of multiple HDACm bands and their rapid resolution to a single band after treating the oocytes with progesterone, indicates a low activity of phosphatases before induction of maturation. However, within a few hours activity becomes high enough to completely dephosphorylate the stored HDACm before GVBD. The only other stage of early development which exhibits such multiple isoforms is mid-blastula (not shown), when there is a global deacetylation of histones that were previously assembled into replicating chromatin (J.T.P.R. and J.S., unpublished). Notice, that the pool of HDACm stored in the GV is not distributed throughout the nucleoplasm but rather is associated with the nuclear envelope in oocytes and cleavage-stage embryos (Ryan et al., 1999). There were previous reports that HDAC activity is associated with nuclear matrix material in immature chicken erythrocytes (Li et al., 1996).

That the stored HDACm in non-injected oocytes is not associated with the endogenous chromatin has been shown in isolated lampbrush chromosomes; they are not immunostained by the same antibodies that immunostain chromosomes from oocytes injected with an excess of in vitro-synthesized HDACm (Ryan et al., 1999). However, overexpression of recombinant HDACm apparently triggers a release from the constraints that anchor the endogenous HDACm on the nuclear envelope, and subsequent binding of HDACm to the chromosomes leads to premature condensation of the

chromosomes (Ryan et al., 1999). This condensation is blocked by low concentrations of trichostatin A (TSA), an specific inhibitor of HDACm-associated histone deacetylase activity (Ryan et al., 1999). Here we have shown that chromatin condensation is associated with a global loss of transcriptional activity and a widespread deacetylation of K12 on histone H4 (Fig. 8). Furthermore, all of these changes (chromatin condensation, transcription inactivation and histone deacetylation) can be prevented by overexpression of HDACm mutated at two phosphorylation sites (S421A and S423A). This striking effect pinpoints the phosphorylation sites required for maximum enzyme activity of HDACm (Ryan et al., 1999) and relates to findings that CK2-mediated phosphorylation promotes both protein-complex formation and enzyme activity of other class 1 HDACs (Pflum et al., 2001; Tsai and Seto, 2002; Sun et al., 2002). Rather than phosphorylation of HDAC directly promoting enzyme activity, our study points to phosphorylation-regulating steps in the association of HDAC with other proteins. This is not only in the formation of enzymatically active complexes, but also in the formation and dissociation of nuclear import complexes.

We thank Bryan Turner for antibodies to the C-terminus of HDACm and lysine 12 of histone H4 and Dirk Görlich for antibodies to *Xenopus* importin-α. This work was supported by a grant from The Wellcome Trust.

References

Adamson, E. D. and Woodland, H. R. (1974). Histone synthesis in early amphibian development: histones and DNA synthesis are not co-ordinated. *J. Mol. Biol.* **88**, 263-285.

Almouzni, G., Khochbin, S., Dimitrov, S. and Wolffe, A. P. (1994). Histone acetylation influences both gene expression and development of *Xenopus laevis*. *Dev. Biol*. **165**, 15837-15844.

Barz, T., Ackermann, K., Dubois, G., Eils, R. and Pyerin, W. (2003). Genome-wide expression screens indicate a global role for protein kinase CK2 in chromatin remodelling. *J. Cell Sci*. **116**, 1563-1577.

Chambers, S. A. M. and Shaw, B. R. (1987). Histone modification accompanying the onset of developmental commitment. *J. Biol. Chem.* **259**, 13458-13463.

de Ruijter, A. J., van Gennip, A. H, Caron, H. N., Kemp, S. and van Kuilenburg, A. B. (2003). Histone deacetylases (HDACs): characterization of the classical HDAC family. *Biochem J.* **370**, 737-749.

Dimitrov, S., Almouzni, G., Dasso, M. and Wolffe, A. P. (1993). Chromatin transitions during early *Xenopus* embryogenesis: changes in histone H4 acetylation and in linker histone type. *Dev. Biol*. **160**, 214-227.

Dilworth, S. M., Black, S. J. and Laskey, R. A. (1987). Two complexes that contain histones are required for nucleosome assembly *in vitro*: role of nucleoplasmin in N1 in *Xenopus* egg extracts. *Cell* **51**, 1009-1018.

Dingwall, C. and Laskey, R. A. (1991). Nuclear targeting sequences – a consensus? *Trends Biochem. Sci*. **16**, 478-481.

Dumont, J. N. (1977). Oogenesis in Xenopus laevis. *J. Morphol*. **136**, 153-180.

Evans, J. P. and Kay, B. K. (1991) Biochemical fractionation of oocytes. *Methods Cell Biol.* **36**, 133-148.

Ikegami, S., Ooe, Y., Shimizu, T., Kasahara, T., Tsuruta, T., Kijima, M., Yoshida, M. and Beppu, T. (1993). Accumulation of multiacetylated forms of histones by trichostatin A and its developmental consequences in early starfish embryos. *Roux's Arch. Dev. Biol*. **202**, 144-151.

Izaurralde, E., Kutay, U., von Kobbe, C., Mattaj, I. W. and Görlich, D. (1997). The asymmetric distribution of the constituents of the Ran system is essential for transport into and out of the nucleus. *EMBO J.* **16**, 6535-6547.

Jans, D. A., Xiao, C-Y. and Lam, M. H. C. (2000). Nuclear targeting signal recognition: a key control point in nuclear transport? *Bioessays* **22**, 532-544.

Kleinschmidt, J. A. and Seiter, A. (1988). Identification of domains involved in nuclear uptake and histone binding of protein N1 of *Xenopus laevis*. *EMBO J.* **7**, 1605-1614.

Kleinschmidt, J. A., Fortkamp, E., Krohne, G., Zentgraf, H. and Franke, W. W. (1985). Co-existence of two different types of soluble histone complexes in nuclei of *Xenopus laevis* oocytes. *J. Biol. Chem.* **260**, 1166-1176.

Kouzarides, T. (2000). Acetylation: a regulatory modification to rival phosphorylation? *EMBO J.* **19**, 1176-1179.

Kuersten, S., Ohno, M. and Mattaj, I. W. (2001). Nucleocytoplasmic transport: Ran, beta and beyond. *Trends Cell Biol.* **11**, 497-503.

Ladomery, M., Lyons, S. and Sommerville, J. (1997). *Xenopus* HDm, a maternally expressed histone deacetylase, belongs to an ancient family of acetyl-metabolising enzymes. *Gene* **198**, 275-280.

Lemaitre, J. M., Geraud, G. and Mechali, M. (1998). Dynamics of the genome during early *Xenopus* development: karyomeres as independent units of replication. *J. Cell Biol.* **142**, 1159-1166.

Li, W., Chen, H. Y. and Davie, J. R. (1996). Properties of chicken erythrocyte histone deacetylase associated with the nuclear matrix. *Biochem. J.* **314**, 631-637.

Marmorstein, R. (2001). Structure of histone deacetylases: insights into substrate recognition and catalysis. *Structure* **9**, 1127-1133.

Peng, H. B. (1991). Solutions and protocols. *Methods Cell Biol.* **36**, 657-662.

Pflum, M. K., Tong, J. K., Lane, W. S. and Schreiber, S. L. (2001). Histone deacetylase I phosphorylation promotes enzymatic activity and complex formation. *J. Biol. Chem.* **276**, 47733-47741.

Rhis, H.-P., Jans, D. A., Fan, H. and Peters, R. (1991). The rate of nuclear cytoplasmic protein transport is determined by the casein kinase II site flanking the nuclear localization sequence of the SV40 T-antigen. *EMBO J.* **10**, 633-639.

Ryan, J., Llinas, A. J., White, D. A., Turner, B. M. and Sommerville, J. (1999). Maternal histone deacetylase is accumulated in the nuclei of *Xenopus* oocytes as protein complexes with potential enzyme activity. *J. Cell Sci*. **112**, 2441-2452.

Sobel, R. E., Cook, R. G., Perry, C. A., Annunziato, A. T. and Allis, C. D. (1995). Conservation of deposition-related acetylation sites in newly synthesized histones H3 and H4. *Proc. Natl. Acad. Sci. USA* **92**, 1237-1241.

Sommerville, J., Baird, J. and Turner, B. M. (1993). Histone H4 acetylation and transcription in amphibian chromatin. *J. Cell Biol*. **120**, 277-290.

Sun, J. M., Chen, H. Y., Moniwa, M., Litchfield, D. W., Seto, E. and Davie, J. R. (2002). The transcriptional repressor Sp3 is associated with CK2-phosphorylated histone deacetylase 2. *J. Biol. Chem.* **277**, 35783-35786.

Tsai, S. C. and Seto, E. (2002). Regulation of histone deacetylase 2 by protein kinase CK2. *J. Biol. Chem.* **277**, 31826-31833.

Turner B. M. (2000). Histone acetylation and an epigenetic code. *Bioessays* **22**, 836-845.

Vancurova, I., Paine, T. M., Lou, W. and Paine, P. L. (1995). Nucleoplasmin associates with and is phosphorylated by casein kinase II. *J. Cell Sci.* **108**, 779-787.

Weis, K. (2002). Nucleocytoplasmic transport: cargo trafficking across the border. *Curr. Opin. Cell Biol.* **14**, 328-335.

Wolffe, A. P. (1994). Nucleosome positioning and modification: chromatin structures that potentiate transcription. *Trends Biochem. Sci.* **19**, 240-244.